

Ferromagnetic nanotubes by atomic layer deposition in anodic alumina membranes

M. Daub, M. Knez, U. Goesele, and K. Nielsch

Citation: *J. Appl. Phys.* **101**, 09J111 (2007); doi: 10.1063/1.2712057

View online: <http://dx.doi.org/10.1063/1.2712057>

View Table of Contents: <http://jap.aip.org/resource/1/JAPIAU/v101/i9>

Published by the [American Institute of Physics](#).

Related Articles

Growth and stability of zinc blende MgS on GaAs, GaP, and InP substrates
Appl. Phys. Lett. **102**, 032102 (2013)

Experimental study of nanofiber production through forcespinning
J. Appl. Phys. **113**, 024318 (2013)

Controllable evaporation of cesium from a dispenser oven
Rev. Sci. Instrum. **83**, 123305 (2012)

Optimal algorithm for spray pyrolysis deposition of TiO₂ films by using an industrial robot
J. Renewable Sustainable Energy **4**, 053126 (2012)

Omnidirectional reflection from nanocolumnar TiO₂ films
J. Appl. Phys. **112**, 084317 (2012)

Additional information on J. Appl. Phys.

Journal Homepage: <http://jap.aip.org/>

Journal Information: http://jap.aip.org/about/about_the_journal

Top downloads: http://jap.aip.org/features/most_downloaded

Information for Authors: <http://jap.aip.org/authors>

ADVERTISEMENT



AIP Advances

Now Indexed in Thomson Reuters Databases

Explore AIP's open access journal:

- Rapid publication
- Article-level metrics
- Post-publication rating and commenting

Ferromagnetic nanotubes by atomic layer deposition in anodic alumina membranes

M. Daub,^{a)} M. Knez, U. Goesele, and K. Nielsch

Max-Planck-Institute for Microstructure Physics, Weinberg 2, D-06120 Halle, Germany

(Presented on 11 January 2007; received 31 October 2006; accepted 18 December 2006; published online 8 May 2007)

In this paper, two methods for the synthesis of magnetic nanotubes inside the pores of anodic alumina membranes by atomic layer deposition (ALD) are compared. The precursors were nickelocene or cobaltocene, and H₂O or O₃. The first method consists of a three-step ALD cycle: First, the sample is exposed to the metal-organic precursor, subsequently to water, and finally, to hydrogen. In the second method, metal oxide is deposited by a conventional two-step ALD cycle. After the ALD process, the sample is reduced under hydrogen atmosphere. The magnetic nanotubes obtained by the second method have a smaller grain size and improved magnetic properties. The magnetic nanotubes with diameters ranging from 35 to 60 nm exhibit a preferential magnetization direction along the nanowire axis. The Ni or Co nanotubes with larger diameters (around 160 nm) show a nearly isotropic magnetic behavior, with the magnetic moments arranged in a vortex state at zero field. © 2007 American Institute of Physics. [DOI: [10.1063/1.2712057](https://doi.org/10.1063/1.2712057)]

I. INTRODUCTION

Patterned magnetic nanostructures are presently the focus of intense investigations because of their scientifically interesting properties and their potential applications in many areas of nanotechnology, such as patterned magnetic media, sensing devices, or magnetic imaging. Ni and Co nanotubes have been fabricated by silanization of polycarbonate or alumina membranes, followed by electrochemical deposition.^{1–3} Co, Fe, CoNiFe/Cu, and Ni nanotubes were produced by pulsed electro-deposition^{4,5} or by dc electrodeposition, adding an amphiphilic triblock copolymer in the electrodeposition solution.⁶ Au/Ni multilayer nanotubes were fabricated by coating alumina walls with Ag nanoparticles and subsequent electrodeposition.⁷ Precursor injection and subsequent hydrogen reduction were used for the fabrication of FePt and FePt/Fe magnetic nanotubes.^{8,9} By wetting the pores of alumina membranes with a polystyrene/poly-*l*-lactide solution containing a metallo-organic precursor and annealing, Co nanotubes were fabricated.¹⁰ Most previous papers report the formation of nanotubes with relatively large diameters (200–300 nm). In addition, these methods do not allow a precise control of the layer thickness and a fine tuning of magnetic properties of the deposited material.

Atomic layer deposition (ALD) offers a very precise control of the growth rate and a very conformal coating on three-dimensional structures. ALD consists of the deposition of thin layers from two different vapor-phase reactants. The substrate is subsequently exposed to the precursor vapor; in each cycle, usually one monolayer or less of the desired material is deposited and the deposition should be repeated several times until the desired layer thickness is reached. Here, we fabricate magnetic nanotubes in porous alumina templates by two different ALD approaches.

II. FABRICATION OF NANOTUBES

Alumina membranes with 100 and 500 nm interpore distance, pore diameters of 35 and 160 nm, and pore lengths of 2–50 μm were fabricated in a two-step anodization process of aluminum.^{11–13} To obtain pore diameters of 55–85 nm, we treated the samples in 5% H₃PO₄ at 30 °C for 30–60 min. The alumina membranes were used as templates for the ALD deposition (Savannah, Cambridge Nanotech) of Ni and Co.

The first method (“reduction during the ALD process”) consists in a three-step deposition cycle: First, the nickelocene (or cobaltocene) vapor is introduced into the deposition chamber and allowed to adsorb at the sample surface. Then, the sample surface is exposed to H₂O vapor to form a layer of metal oxide from the metallo-organic complex. Finally, H₂ is used to reduce the formed oxide layer. Between each step, the ALD chamber is purged in order to avoid interactions in vapor phases.

The second method (“reduction after the ALD process”) consists of only two steps: First, the nickelocene or cobaltocene vapor forms a submonolayer on the sample surface. Then, O₃ is introduced into the ALD chamber to react with the adsorbed layer. After the ALD process, the sample with the metal oxide coating is transferred into an oven and reduced at 400 °C under Ar+5% H₂ atmosphere for 5 h.

For Ni, the deposition temperature ranged between 270 and 330 °C (the maximum temperature of our ALD reactor) and for Co, between 240 and 330 °C at 2×10^{-1} Torr. We used nickelocene (NiCp₂) or cobaltocene (CoCp₂), both from Strem Chemicals, as first precursors. The precursor temperature was, in both cases, 90 °C. Pulsing time of 1 s, exposure time of 30 s, and purging time [Ar gas, flow rate of 10 SCCM (SCCM denotes cubic centimeter per minute at STP)] of 30 s were used for all ALD cycles.

For the scanning electron microscopy (SEM) and magnetic measurements, the alumina surface was treated by an ion milling process to remove the deposited film from the top

^{a)}Electronic mail: mdaub@mpi-halle.de

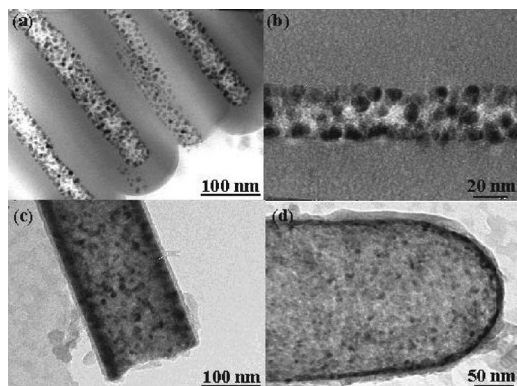


FIG. 1. (a) $\text{TiO}_2/\text{Ni}/\text{TiO}_2$ nanotubes obtained with the first method (“reduction during the ALD process”). (b) Ni tubes deposited with the second method (“reduction after the ALD process”).

sample surface. For a higher stability of the nanotubes, a better contrast in the SEM, and to prevent damaging of the nanotubes by the etching solution, we deposited TiO_2 ¹⁷ by ALD as follows: first, a layer of TiO_2 was deposited in the alumina membrane, then, e.g., Ni deposition was performed as above, and finally, a second thin layer of TiO_2 was used to cover the Ni tubes. For transmission electron microscopy (TEM) measurements, the $\text{TiO}_2/\text{Ni}/\text{TiO}_2$ tubes were released by etching the membrane with 1M NaOH and washing several times with purified water. A droplet of the nanotube-containing suspension was placed onto copper grids with carbon film and dried.

III. RESULTS AND DISCUSSION

We investigated the morphology of the nanotubes by SEM and TEM measurements. Figure 1 shows transmission electron micrographs of $\text{TiO}_2/\text{Ni}/\text{TiO}_2$ tubes with method 1 [800 cycles ALD at 330 °C, Figs. 1(a) and 1(b)] and with method 2 [500 ALD cycles at 330 °C, Figs. 1(c) and 1(d)]. The layer thickness is about the same range, 11–12 nm. The tubes that we studied by TEM had two different sets of diameters: 35 or 160 nm. The length of the pores presented in Fig. 1 is almost the same (10 μm).

For nanotubes obtained by the first method, the measured grain size was 12–15 nm. For nanotubes fabricated by the second method, the grain size was less than 5 nm, probably due to the fact that we grow, in this case, an oxide layer on another oxide layer. In the first method, we reduce the oxide to metal in each cycle, and this might lead to increased granularity.

The morphology of the multilayer $\text{TiO}_2/\text{Ni}/\text{TiO}_2$ tubes is also confirmed by SEM measurements. The Ni tubes presented in Fig. 2 were obtained by 500 ALD cycles with O_3 (method 2). The first TiO_2 layer has a thickness of about 10 nm, and the second TiO_2 layer of about 5 nm. The Ni tube thickness is 11–12 nm. The pore diameter is about 160 nm and the length is about 10 μm . In Fig. 2(a), the alumina membrane was completely etched away by NaOH. In this case, the $\text{TiO}_2/\text{Ni}/\text{TiO}_2$ top layer was not removed by ion milling, so that the interconnecting layer was preserved. In Fig. 2(b), the top surface was removed and the trilayer structure can be observed from a top-view perspective.

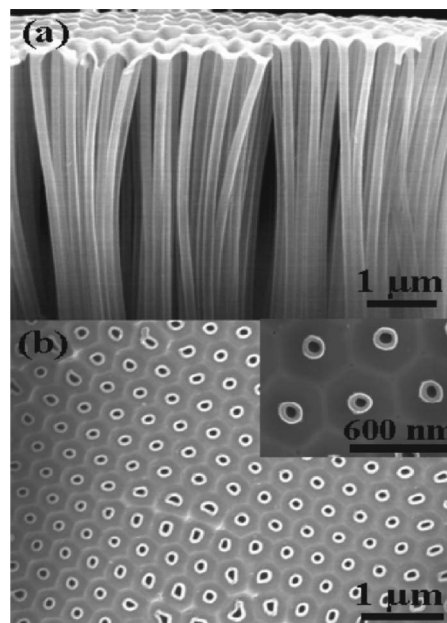


FIG. 2. $\text{TiO}_2/\text{Ni}/\text{TiO}_2$ nanotubes obtained using the second method (reduction after the ALD process). The tubes shown in (a) are removed from the alumina membrane with a solution of 1M NaOH (a). The tubes in (b) are embedded in the membrane; the ferromagnetic layer on the top surface have been removed by ion milling.

Recently, ALD processes have been developed for magnetic thin films.¹⁴ Due to the low reactivity of molecular hydrogen, most processes for transition metals, e.g., Ni and Co, based on the reaction of H_2 and a metal-organic precursor, are rather slow (0.04–0.12 $\text{\AA}/\text{cycle}$). The deposition rates for metal oxides obtained by ALD are usually between 0.2 and 1.5 $\text{\AA}/\text{cycle}$.^{14–16} We obtained very uniform and conformal nanostructures with deposition rates of 0.22–0.3 $\text{\AA}/\text{cycle}$ by method 2.

The magnetic properties of Ni nanotubes with different diameters and lengths were measured with a superconducting quantum interference device (SQUID) magnetometer. Hysteresis loops for samples obtained by the two methods (pore diameter of 35 nm, pore length of 30 μm , and Ni layer thickness of around 12 nm) are presented in Fig. 3. Ni nanotubes obtained by the first method show very small coercivities (<30 Oe for both directions: parallel and perpendicular to the tube axis). Typical coercivities for samples obtained by

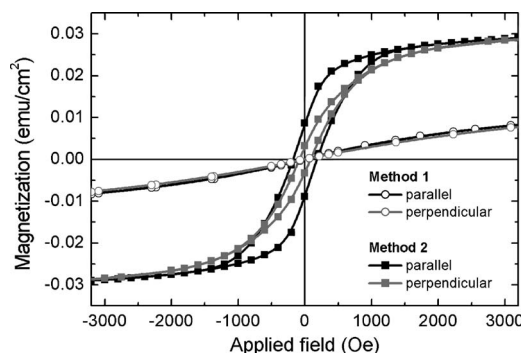


FIG. 3. Hysteresis loops for Ni nanotubes embedded in the alumina membrane, for the two different methods; the applied magnetic field is parallel to the tube axis.

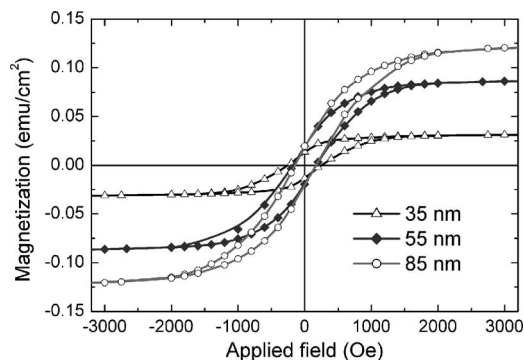


FIG. 4. Hysteresis cycles (parallel direction) for Ni nanotubes obtained with the second method as a function of pore diameter. The Ni layer thickness is the same (11–12 nm).

method 2 are 190 Oe for the parallel configuration and 90 Oe for the perpendicular configuration ($1 \text{ Oe} = 10^3/4\pi \text{ A m}^{-1}$). The coercivities measured for Co nanotubes (method 2, similar deposition parameters and dimensions) are 550 Oe for the parallel direction and 390 Oe for the perpendicular direction. For pore diameters of around 160 nm, the Ni and Co nanotubes showed a nearly isotropic behavior, with coercivities in both measurement configurations of around 100 Oe (for Ni) and 580 Oe (for Co). All measured coercivity values are in the same range as values from literature.^{1,6} As a comparison, the coercivity values for bulk are much smaller ($<10 \text{ Oe}$ for Ni; around 10 Oe for Co). Due to the shape anisotropy, the nanotubes with smaller diameters (around 35 nm) show enhanced coercivities and anisotropic magnetic behavior. For these samples, the remanent magnetization for the applied field parallel to the tube axis is larger than that for the perpendicular direction, indicating that the easy axis of magnetization is oriented along the nanotube axis. The preferential arrangement of the magnetic moments is the parallel (ferromagnetic) configuration for smaller diameters ($<80 \text{ nm}$) and a vortex state for the larger diameter nanotubes ($>100 \text{ nm}$).¹⁸ The influence of the pore diameter or the layer thickness on the magnetic properties was also investigated. Figure 4 shows the hysteresis cycles for three different samples obtained with method 2 (diameters of 35, 55, and 85 nm; interpore distance of 100 nm; and pore length of around $30 \mu\text{m}$). All three samples were deposited with the same number of ALD cycles, corresponding to 11–12 nm Ni thickness. We observed that when the pore diameter decreases, the coercivity and the remanence increase (and the saturation magnetization decreases). Figure 5 presents the results concerning the influence of the Ni layer thickness on the magnetic nanotube behavior. We used alumina membranes with 35 nm pore diameter and 100 nm interpore distance. As expected, increasing the number of ALD cycles (150, 300, and 500 cycles, corresponding to 3–4, 6–7, and 11–12 nm thickness) leads to an increase in the saturation magnetization and coercivity.

IV. CONCLUSIONS

Ni and Co nanotubes were produced in alumina membranes by atomic layer deposition. Nickelocene or cobal-

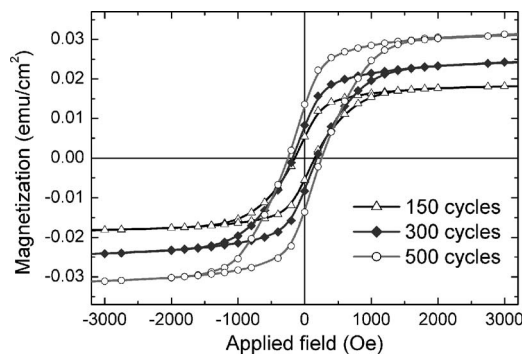


FIG. 5. Hysteresis loops (parallel direction) for Ni nanotubes obtained by the second method, for different Ni layer thickness: 3–4 nm (150 cycles), 6–7 nm (300 cycles), and 11–12 nm (500 cycles). The samples have the same diameter (35 nm) and pore length ($30 \mu\text{m}$).

tocene were used as first precursors, and the influence of H_2O or O_3 as second precursors was investigated. The deposition of metal oxide with O_3 and subsequent reduction lead to a very fine grain structure of the ferromagnetic material. Atomic layer deposition offers a very precise control of layer growth and a high degree of flexibility in the fabrication of three dimensional nanostructures.

ACKNOWLEDGMENTS

The authors appreciate the financial support by the German Ministry of Science and Education, BMBF, via Research Contract No. FKZ 03N8701. The authors thank J. Escrig from Departamento de Fisica, Universidad de Santiago de Chile, Chile, for useful discussions on the interpretation of magnetic results.

- ¹J. Bao, C. Tie, Z. Xu, Q. Zhou, D. Shen, and Q. Ma, *Adv. Mater. (Weinheim, Ger.)* **13**, 1631 (2001).
- ²S. Xue, C. Cao, and H. Zhu, *J. Mater. Sci.* **41**, 5598 (2006).
- ³J. Bao, Z. Xu, J. Hong, X. Ma, and Z. Lu, *Scr. Mater.* **50**, 19 (2004).
- ⁴G. Tourillon, L. Pontonnier, J. P. Levy, and V. Langlais, *Electrochem. Solid-State Lett.* **3**, 20 (2000).
- ⁵D. M. Davis, M. Moldovan, D. P. Young, M. Henk, X. Xie, and E. J. Podlaha, *Electrochem. Solid-State Lett.* **9**, C153 (2006).
- ⁶F. Tao, M. Guan, Y. Jiang, J. Zhu, Z. Xu, and Z. Xue, *Adv. Mater. (Weinheim, Ger.)* **18**, 2161 (2006).
- ⁷W. Lee, R. Scholz, K. Nielsch, and U. Goesele, *Angew. Chem., Int. Ed.* **44**, 6050 (2005).
- ⁸Y. C. Sui, R. Skomski, K. D. Sorge, and D. J. Sellmyer, *J. Appl. Phys.* **95**, 7151 (2004).
- ⁹H. L. Su, S. L. Tang, N. J. Tang, R. L. Wang, M. Lu, and Y. W. Du, *Nanotechnology* **16**, 2124 (2005).
- ¹⁰K. Nielsch, F. J. Castano, C. A. Ross, and R. Krishnan, *J. Appl. Phys.* **98**, 034318 (2005).
- ¹¹K. Nielsch, J. Choi, K. Schwirn, R. B. Wehrspohn, and U. Goesele, *Nano Lett.* **2**, 677 (2002).
- ¹²K. Nielsch, F. J. Castano, S. Matthias, W. Lee, and C. A. Ross, *Adv. Eng. Mater.* **7**, 217 (2005).
- ¹³B. S. Lim, A. Rahtu, and R. G. Gordon, *Nat. Mater.* **2**, 749 (2003).
- ¹⁴J. Chae, H.-S. Park, and S.-w. Kang, *Electrochem. Solid-State Lett.* **5**, C64 (2002).
- ¹⁵M. Utriainen, M. Kröger-Laukkanen, L.-S. Johansson, and L. Niinisto, *Appl. Surf. Sci.* **157**, 151 (2000).
- ¹⁶M. Utriainen, M. Kröger-Laukkanen, L. Niinisto, *Mater. Sci. Eng., B* **54**, 98 (1998).
- ¹⁷M. Knez, A. Kadri, C. Wege, U. Goesele, H. Jeske, and K. Nielsch, *Nano Lett.* **6**, 1172 (2006).
- ¹⁸J. Escrig, P. Landeros, D. Altbir, E. E. Vogel, and P. Vargas, *J. Magn. Magn. Mater.* **308**, 233 (2007).